to detect the shifted lines in the complex species responsible for the observed effects.

The scalar coupling constants obtained for the Ni–H$_2$O interactions (Table VI) are similar to those reported for more dilute solutions containing aquonickel ions. Our values are, however, somewhat higher than

the more recent ones. This suggests that Connick and Fiat's[13] report of four-coordination for the Ni(II) aquo ion may be at least partly a consequence of the high salt concentration used in their direct shift measurements.

(13) R. E. Connick and D. E. Fiat, *J. Chem. Phys.*, **44**, 4103 (1966).

Magnetic Exchange in Transition Metal Complexes. IV.[1a]
Linear Trimeric Bis(acetylacetonato)nickel(II)

BY A. P. GINSBERG, R. L. MARTIN,[1b] AND R. C. SHERWOOD

The magnetic properties of the linear trimeric cluster [Ni$_3$(acac)$_6$] have been measured from room temperature (296°K) down to 0.365°K. At room temperature, the normal value of 3.23 BM per Ni^{2+} ion is found for the effective magnetic moment corresponding to octahedrally coordinated nickel(II). As the temperature is lowered, μ_{eff} (corrected for a small Curie–Weiss constant, $\theta = -0.2°$, due to weak lattice antiferromagnetism) increases monotonically until a constant value of 4.1 ± 0.1 BM is reached below about 10°K. These results, together with magnetization curves at 1.6 and 4.2°K, demonstrate that the six e$_g$ electrons on the three Ni atoms are ferromagnetically coupled, the ground molecular spin state for the trimer being $S = 3$ (*i.e.*, six spins parallel). Comparison of our results with an extension of Kambe's theory for the susceptibility of a magnetically isolated exchange-coupled trimer indicates that adjacent Ni atoms in the linear triad have the positive coupling constant $J = +37°$ ($\equiv +26$ cm^{-1}) while the terminal Ni atoms have the negative value $J_{31} = -10.3°$ ($\equiv -7$ cm^{-1}). The opposing signs for these interactions are shown to be consistent with current views of superexchange. Nickel(II) acetylacetonate provides the first example of ferromagnetic interaction in an isolated cluster.

Introduction

Bis(acetylacetonato)nickel(II) provides an extremely interesting example of a compound in which the crystal lattice is built up of magnetically isolated linear triads of transition metal atoms, with two unpaired e$_g$ spins per atom. Theoretical considerations suggest that the magnetic properties of such an arrangement of unpaired spins might exhibit at least two novel features not previously observed in an isolated cluster complex: (1) There can be two different, nonzero, exchange integrals for a linear trimer molecule, one between adjacent metal atoms and the other between the terminal atoms. (2) The exchange integral between the adjacent Ni atoms may be positive (ferromagnetic).

Our measurements show that the magnetic susceptibility of [Ni$_3$(acac)$_6$] is indeed characterized by both of these features.[2]

The structure[3] of [Ni$_3$(acac)$_6$] is shown in Figure 1. Nearly octahedral coordination of each nickel ion in the linear trimeric molecule results from the sharing of triangular faces of adjacent octahedra. An acetylacetonato oxygen is situated at each apex of the linear triad of fused octahedra. The intramolecular Ni–Ni

distances are 2.882 and 2.896 Å. There are no atomic bridges between molecules in the crystal lattice, and the closest intermolecular Ni–Ni distance is ~8 Å. Consequently, intermolecular spin–spin coupling due to both exchange and dipole–dipole forces is expected to be very weak. The trimer molecules should behave as if magnetically isolated from each other at all but the very lowest temperatures.

Theory

We shall discuss the magnetic susceptibility of [Ni$_3$(acac)$_6$] in terms of the usual Heisenberg–Dirac–Van Vleck spin-coupling Hamiltonian first used by Kambe[4] for this purpose. For an isolated linear trimer, this Hamiltonian is

$$H = -2J[(\hat{S}_1 \cdot \hat{S}_2) + (\hat{S}_2 \cdot \hat{S}_3)] - 2J_{31}(\hat{S}_3 \cdot \hat{S}_1) \quad (1)$$

J is the exchange integral between adjacent nickel atoms (1,2 and 2,3) in the trimer, and J_{31} is the exchange integral between the two terminal nickel atoms (3,1) within the trimer. The $\hat{S}_i$ are spin angular momentum operators. For a system with two unpaired spins on each metal atom, the eigenvalues of (1) are given in Table I, where S' is the total spin of the trimer and S^* is the total spin of the two terminal atoms.[4] Figure 2, which may be referred to as a spin-correlation diagram, shows how the ordering of the spin levels depends on the sign of J and J_{31} and on their relative magnitudes. The diagram is drawn for

(1) (a) Part III: A. P. Ginsberg, E. Koubek, and H. J. Williams, *Inorg. Chem.*, **5**, 1656 (1966); (b) on leave from the Department of Inorganic Chemistry, University of Melbourne, Melbourne, Australia.
(2) Preliminary communication: A. P. Ginsberg, R. L. Martin, and R. C. Sherwood, *Chem. Commun.*, 856 (1967).
(3) G. J. Bullen, R. Mason, and P. Pauling, *Inorg. Chem.*, **4**, 456 (1965).
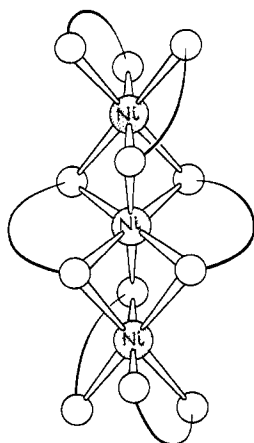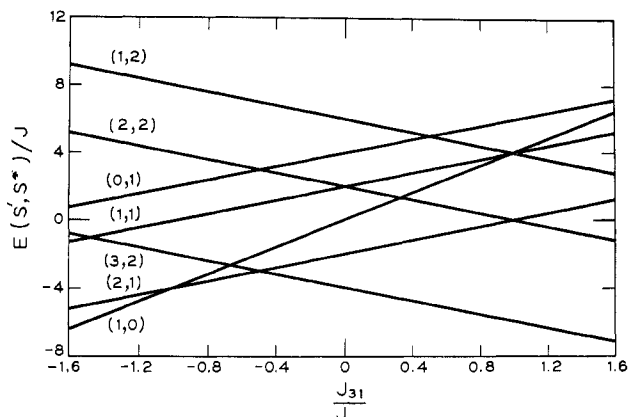(4) K. Kambe, *J. Phys. Soc. Japan*, **5**, 48 (1950).

Figure 1.—Molecular structure of nickel(II) acetylacetonate.

TABLE I

THE ENERGY LEVELS INTO WHICH THE MOLECULAR GROUND
STATE OF $[Ni_3(acac)_6]$ IS SPLIT BY INTERACTION BETWEEN THE
UNPAIRED SPINS ON THE THREE Ni ATOMS

(S',S^*)	$E(S',S^*)$	(S',S^*)	$E(S',S^*)$
(3,2)	$-4J - 2J_{31}$	(1,1)	$2J + 2J_{31}$
(2,2)	$+2J - 2J_{31}$	(1,0)	$4J_{31}$
(2,1)	$-2J + 2J_{31}$	(0,1)	$4J + 2J_{31}$
(1,2)	$6J - 2J_{31}$		

Figure 2.—Spin-correlation diagram for a cluster of three metal
atoms, each with spin $S = 1$.

the case that J is positive, so that the change in sign along the abscissa is due to the change in sign of J_{31}. For negative J the diagram is simply inverted. It is evident that when J is positive the trimer ground state is always paramagnetic, but its spin depends on the value of J_{31}/J. When J is negative, the ground state is diamagnetic only for $0.5 < J_{31}/J < 2$; otherwise, it is paramagnetic. In particular, when J is negative and $J_{31} = 0$, the trimer ground state has a total spin of 1 and is not diamagnetic as implied by some authors.[5]

The magnetic susceptibility of $[Ni_3(acac)_6]$ is found as the mean of the susceptibilities of the individual spin levels, each weighted by its degeneracy and by the appropriate Boltzmann factor. After dividing by 3 to obtain the susceptibility per g-atom of Ni, the result is

(5) B. N. Figgis and J. Lewis, *Progr. Inorg. Chem.*, **6**, 91 (1964).

$$\frac{g^2\chi_A'T}{K} = \mu_{eff}^2 =$$

$$\frac{2K}{3}\left[\frac{\begin{array}{l}42e^{2(2x+y)} + 15e^{2(y-x)} + 15e^{2(x-y)} + \\ \qquad 3e^{2(y-3x)} + 3e^{-2(x+y)} + 3e^{-4y}\end{array}}{\begin{array}{l}7e^{2(2x+y)} + 5e^{2(y-x)} + 5e^{2(x-y)} + 3e^{2(y-3x)} + \\ \qquad 3e^{-2(x+y)} + 3e^{-4y} + e^{-2(2x+y)}\end{array}}\right]$$

$$(2)$$

where

$$x = J/kT$$

$$y = J_{31}/kT$$

and

$$K = \frac{g^2N\beta^2}{3k}$$

Since the spin energy levels in Figure 2 frequently cross as J_{31}/J is varied, and since the trimer ground state can have several different values of the total spin, eq 2 will behave in a variety of different ways depending on the values of J and J_{31}/J. This is illustrated in Figure 3 which shows computer-drawn plots of eq 2 in the form of μ_{eff} per Ni atom *vs.* the reduced temperature kT/J for different values of J_{31}/J.

Experimental Section

Ni(acac)$_2$·2CH$_3$OH was prepared according to a procedure in the literature.[6] Methanol was removed from the product by heating it for several hours at 60° and 1 mm. Recrystallization from dry *n*-hexane under nitrogen gave the trimer. *Anal.* Calcd for NiC$_{10}$H$_{14}$O$_4$: Ni, 22.84; C, 46.75; H, 5.49; O, 24.91. Found: Ni, 22.73; C, 46.62; H, 5.32; O, 25.00. The *d* spacings and intensities of the X-ray powder pattern lines of this compound matched those calculated from the lattice constants and structure factors reported in ref 3.

Magnetic susceptibility measurements were made between 1.5°K (pumped helium) and 300°K with a null-coil pendulum magnetometer.[7] The instrument had been calibrated with a sphere of Johnson and Matthey spectroscopically pure nickel and further checked with a sample of Mohr's salt. Temperatures from 300 to 70°K were measured with a copper–constantan thermocouple, and from 70 to 4.2°K with a carbon resistor. Below 4.2°K the temperature was determined from the helium vapor pressure. Samples weighing ∼0.5 g were used and were contained in a small Teflon capsule into which they were compressed by a tight-fitting Teflon piston. The instrument correction curve was run with the empty Teflon capsule and piston positioned in the magnetometer coil. A magnetization curve determined at 1.59°K showed that for field strengths above about 2500 Oe the susceptibility was field dependent. Measurements were therefore made at 2400 Oe up to 10°K, at which point the susceptibility determined at 2400 Oe was the same as that at our highest magnetometer field strength, namely, 15,300 Oe. Measurements were continued at the latter field strength up to room temperature.

The field dependence of the susceptibility of $[Ni_3(acac)_6]$ was determined to 50,000 Oe at 1.1 and 4.2°K by observing the integrated voltage of a pair of pickup coils as the sample is moved from one coil to the other in a constant applied magnetic field. The apparatus is calibrated by means of a nickel sphere of known

(6) R. G. Charles and M. A. Pawlikowski, *J. Phys. Chem.*, **62**, 440 (1958).

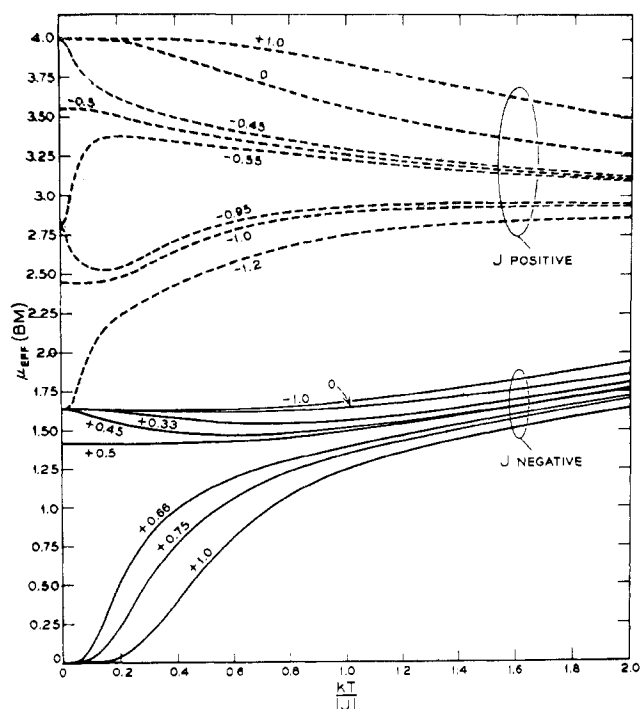(7) R. M. Bozorth, H. J. Williams, and D. E. Walsh, *Phys. Rev.*, **103**, 572 (1956).

Figure 3.—Theoretical dependence of μ_{eff} (BM) per Ni atom upon the reduced temperature kT/J for several values of J_{31}/J.

saturation magnetization and fields up to 50,000 Oe are produced by means of a superconducting solenoid.

Measurements were also made of the ac susceptibility of [Ni$_3$-(acac)$_6$] by placing the polycrystalline sample in the tank coil of an oscillator normally used for detecting superconductivity. The relative ac susceptibility in zero field (detected as a frequency shift in the resonant circuit) was determined as a function of temperature between 0.365 and 4.2°K by this method.

Results

Our measurements of the field-independent susceptibility of [Ni$_3$(acac)$_6$] between 1.5 and 300°K are given in Table II as χ_A', the susceptibility per Ni atom. A diamagnetic correction[8] ($\chi_d = -106 \times 10^{-6}$ cm^3 g-atom^{-1}) is included. The results are shown in Figure 4 as plots of $1/\chi_A'$ and $\mu_{eff} = 2.8273[(\chi_A' - N\alpha)T]^{1/2}$ vs. T. The TIP correction[9] $N\alpha = +230 \times 10^{-6}$ cm^3 g-atom^{-1}.

The low-temperature ac measurements show no indication of any anomaly in the susceptibility curve down to 0.365°K. A Curie–Weiss law is followed with a Weiss constant $\theta = -0.2°$ in the range 1.5–0.365°K. At the latter temperature $\mu_{eff} = 2.58$ BM.

Figure 5 shows the magnetization curves determined at 4.2 and 1.1°K. The ordinate in this plot, $\langle\mu\rangle$ per trimer, is the z component of the magnetic moment per trimer molecule.

Discussion

At 296°K, $\mu_{eff} = 3.23$ BM per Ni atom. As the temperature is decreased, μ_{eff} gradually increases until at 4.3°K a maximum value of 4.1 BM is reached. Comparison with the theoretical curves in Figure 3

(8) P. W. Selwood, "Magnetochemistry," 2nd ed, Interscience Publishers, Inc., New York, N. Y., 1956, pp 78, 92.

(9) See, for example, C. J. Ballhausen, "Introduction to Ligand Field Theory," McGraw-Hill Book Co., Inc., New York, N. Y., 1962, p 142.
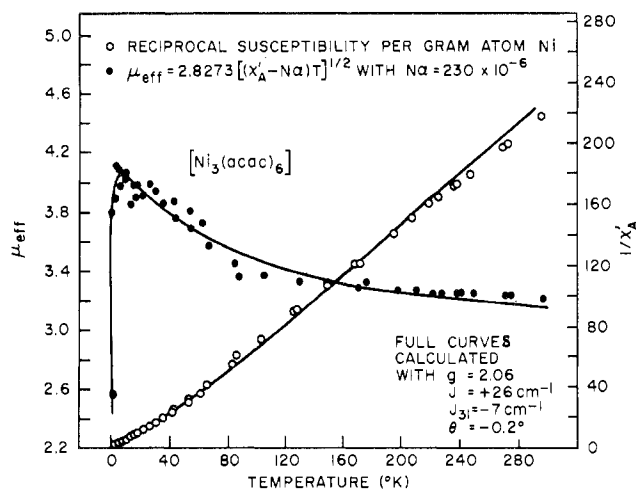
Figure 4.—Temperature dependence of μ_{eff} (BM) per Ni atom and $1/\chi_A'$ for [Ni$_3$(acac)$_6$].

TABLE II

EXPERIMENTAL VALUES OF THE FIELD-INDEPENDENT SUSCEPTIBILITY PER Ni ATOM OF [Ni$_3$(acac)$_6$] BETWEEN 1.5 AND 300°K WHERE $\mu_{eff} = [(\chi_A' - N\alpha)T]^{1/2}$

| T, °K	$10^6\chi_A'$, cm^3 g-atom^{-1}	μ_{eff}, BM	T, °K	$10^6\chi_A'$, cm^3 g-atom^{-1}	μ_{eff}, BM
1.6	1,130,000	3.8$_0$	66.3	24,400	3.5$_8$
1.95	951,000	3.8$_5$	84.0	18,100	3.4$_6$
4.3	493,000	4.1$_2$	87.0	16,600	3.3$_7$
5.9	356,000	4.1$_0$	104.0	14,000	3.3$_8$
7.3	273,000	3.9$_9$	127.5	11,150	3.3$_4$
10.1	201,000	4.0$_3$	129.0	11,050	3.3$_4$
10.4	199,500	4.0$_7$	150.5	9,370	3.3$_2$
13.8	135,000	3.8$_6$	151.0	9,290	3.3$_1$
16.0	125,000	3.9$_9$	169.0	8,270	3.3$_0$
17.1	112,500	3.9$_2$	173.5	8,240	3.3$_3$
19.0	105,000	3.9$_9$	196.0	7,110	3.2$_8$
21.7	88,600	3.9$_2$	209.0	6,660	3.2$_8$
26.9	74,300	3.9$_9$	220.5	6,270	3.2$_6$
31.0	63,100	3.9$_5$	226.5	6,120	3.2$_7$
36.0	52,100	3.8$_6$	237.0	5,860	3.2$_7$
43.0	44,000	3.8$_8$	239.0	5,830	3.2$_7$
43.7	40,900	3.7$_7$	248.5	5,620	3.2$_7$
53.7	34,200	3.8$_2$	270.5	5,110	3.2$_5$
54.0	31,900	3.7$_0$	273.5	5,050	3.2$_5$
62.0	28,400	3.7$_4$	296.0	4,650	3.2$_3$
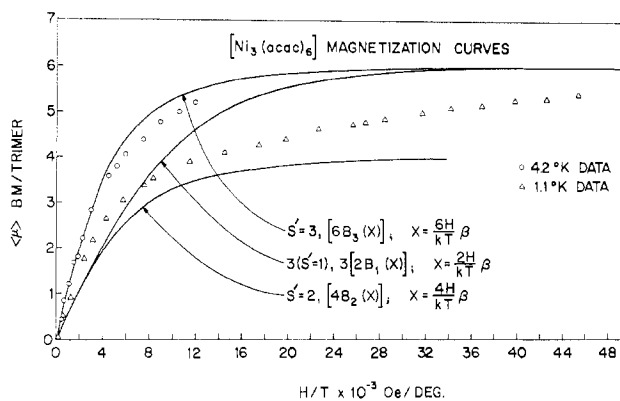
Figure 5.—Magnetization curves for [Ni$_3$(acac)$_6$]. Full curves are calculated Brillouin functions. Experimental data are designated by circles (4.2°K) and triangles (1.1°K).

indicates that J must be positive; *i.e.*, the spins of adjacent Ni atoms are ferromagnetically coupled. An $S' = 3$ state of the trimer, in which all six e_g spins are coupled parallel, corresponds to a μ_{eff} of 4.2 BM per Ni atom for $g = 2.1$. Hence, our results show that by 4.3°K the trimer molecules are largely in an $S' = 3$ spin state.

Below 4.3°K, μ_{eff} decreases with decreasing temperature. The possibility that this is an intramolecular phenomenon, *i.e.*, that an $S' = 2$ or 1 spin level lies below the $S' = 3$ level, is eliminated by a comparison of the results with eq 2 for appropriate values of J and J_{31}. A reasonable interpretation is that the decrease in moment below 4°K is due to the combined effects of a small zero-field splitting of the $S' = 3$ state and a very weak-lattice antiferromagnetic interaction between the trimer molecules. This is consistent with the low-temperature ac susceptibility measurements and also with the magnetization curves in Figure 5.

The solid curves in Figure 5 are plots of the Brillouin function

$$\langle\mu\rangle = 2S'B_{S'}(x) =$$
$$2S'\left[\frac{2S'+1}{2S'}\coth\left(\frac{2S'+1}{2S'}\right)x - \frac{1}{2S'}\coth\frac{x}{2S'}\right]$$

where $x = 2S'\beta H/kT$. At 4.2°K, where the effects of the zero-field splitting and lattice antiferromagnetism are very small, the sample is only slightly more difficult to magnetize than if it followed the theoretical curve for an $S' = 3$ state, but at 1.1°K, where these effects become appreciable, the divergence from the theoretical curve is large. Also shown in Figure 5 are the theoretical curves for an $S' = 2$ trimer ground state and that for three uncoupled Ni atoms; both of these are clearly inconsistent with the experimental data.

In order to permit eq 2 to take account of the low-temperature decrease in μ_{eff}, the right-hand side was multiplied by the ratio $T/(T + 0.2)$. The least-squares best fit of this modification of eq 2 to the experimental μ_{eff} is found for $g = 2.06$, $J = +37°$ ($\equiv +26$ cm^{-1}), and $J_{31} = -10.3°$ ($\equiv -7$ cm^{-1}). Figure 4 shows the comparison between experiment and theory; the agreement is quite satisfactory. The ordering of the spin levels required by the values found for J and J_{31} may be read from Figure 2.

In summary, we consider that our results strongly support the following conclusions: (1) the spins on adjacent Ni atoms of [Ni$_3$(acac)$_6$] interact ferromagnetically with an exchange integral of about 26 cm^{-1}; (2) the spins on the two terminal Ni atoms of [Ni$_3$-(acac)$_6$] interact antiferromagnetically with an exchange integral about one-fourth that between adjacent Ni atoms; (3) the molecular ground state of the trimer has total spin $S' = 3$ corresponding to six electrons with their spins parallel.

A qualitative understanding of the different signs of J and J_{31} is possible if we consider the different paths for exchange between the metal atoms. Following the more recent viewpoint of Anderson,[10,11] we

consider three principal contributions to the exchange integral.

1. Superexchange.—This is defined by Anderson as the exchange effect due to the direct transfer of an electron from cation to cation *via* d wave functions which have been "expanded" by admixture with ligand functions of the appropriate symmetry. For transfer to occur the d orbitals must overlap and the spin of the transferred electron must be antiparallel to that of the electron on the acceptor cation (Pauli principle). As a result the effect is always antiferromagnetic.

2. True Direct Exchange.—Anderson uses this term to describe the exchange effect between two unpaired spins in mutually orthogonal orbitals. It is always ferromagnetic and arises from the Coulomb repulsion of the overlap charge.

3. Electron Transfer Plus Intraatomic Direct Exchange.—This is a second ferromagnetic exchange mechanism which arises when electron transfer is associated with intraatomic direct exchange effects on either the donor or acceptor cations. This interaction is encountered when a half-filled orbital overlaps either an empty orbital or a completely filled orbital on an atom which also contains an unpaired spin in an orbital orthogonal to the one being overlapped.

In [Ni$_3$(acac)$_6$] the Ni–O–Ni angles vary between 76.5 and 89.3°. In the following discussion we consider an idealized situation in which the Ni atoms are linked by 90° Ni–O–Ni bridges. This simplification is necessary in order to apply Anderson's theory in its current stage of development.

Figure 6 shows the orientation of the relevant orbitals. Antiferromagnetic superexchange between adjacent e_g orbitals, in which the unpaired spins are located, should be small (Figure 6a). This is because the only orbital which mixes with both adjacent e_g orbitals is the oxygen 2s, and the effect of this in expanding the magnetic orbitals should be rather small.[11] True direct exchange between Ni atoms will not take place because the unpaired spins are not in mutually orthogonal orbitals. However, because of the symmetry properties of the e_g–p–t_{2g} orbitals arranged at 90° (Figure 6b), a ferromagnetic term arises from electron transfer plus intraatomic direct exchange. Thus, overlap of either $d_{x^2-y^2}$–p$_x$–d$_{xy}$ or d_{xy}–p$_y$–d$_{x^2-y^2}$ sets provides a pathway for unpaired spin density, initially located in e_g orbitals, to be delocalized into the adjoining t_{2g} subset. Intraatomic coupling between the t_{2g} and e_g subsets centered on each Ni atom then couples the two Ni atoms ferromagnetically.

For the exchange coupling between the two terminal Ni atoms (*i.e.*, J_{31}), the only pathway evident is *via* the π system of the two acetylacetone groups which bridge them. If the orientation of the p$_\pi$ orbitals is chosen as shown in Figure 7, then there is a finite overlap between this π system and the half-filled d$_{x^2-y^2}$ orbitals of the terminal Ni atoms. The resulting

(10) P. W. Anderson, *Phys. Rev.*, **115**, 2 (1959).

(11) P. W. Anderson in "Magnetism," Vol. 1, G. T. Rado and H. Suhl, Ed., Academic Press Inc., New York, N. Y., 1963, Chapter 2.
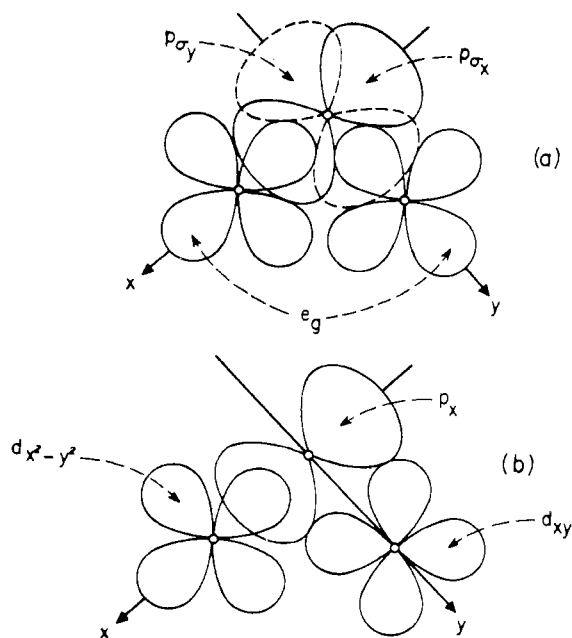
Figure 6.—The orientation of $p\sigma_x$ and $p\sigma_y$ orbitals on oxygen with respect to e_g and t_{2g} orbitals on two nickel atoms arranged at right angles.

interaction must be antiferromagnetic superexchange. It is also possible to orient the p_π orbitals to overlap the d_{xy} orbitals on the terminal Ni atoms. However,
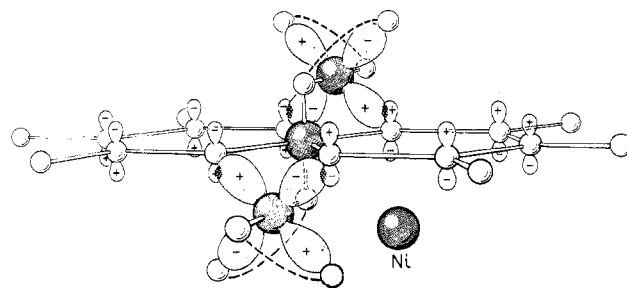

Figure 7.—Superexchange pathway between e_g orbitals centered on atoms Ni_1 and Ni_3 and the π system of the bridging acetylacetonate ligands.

since these are both filled orbitals, there is no exchange effect. There is no orientation of the π system which will result in the simultaneous overlap of the $d_{x^2-y^2}$ orbital of one terminal Ni atom with the d_{xy} of the other. Accordingly, ferromagnetic coupling by electron transfer plus intraatomic direct exchange is precluded. The net interaction between the end members of the trimer is therefore expected to be antiferromagnetic as is observed experimentally.

Acknowledgments.—The authors are indebted to G. W. Hull for measurements of ac susceptibility and to K. Andres for magnetization data at field strengths exceeding 15,000 Oe.

Rates and Mechanism of Substitution Reactions of Sterically Hindered Palladium(II) Complexes

By JOHN B. GODDARD and FRED BASOLO

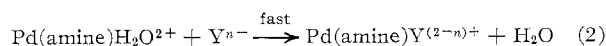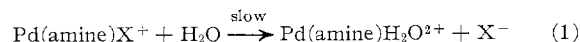The preparation and characterization of the complexes Pd(dien)SO₃, Pd(Et₄dien)SO₃, Pd(Et₄dien)S₂O₃, Pd(MeEt₄dien)-S₂O₃, Pd(Me₅dien)S₂O₃, [Pt(Et₄dien)NH₃][PtCl₄]·H₂O, and [Pt(Et₄dien)NH₃]Cl₂[1] are described, as well as the *in situ* preparation of [Pd(Et₄dien)H₂O](ClO₄)₂. In these complexes, the amine is tridentate and the other ligand is unidentate. The kinetics of the reaction of sulfite ion with [Pd(Et₄dien)Br]Br and of thiosulfate ion with [Pd(Et₄dien)Br]Br, [Pd(Me₅dien)-Cl]PF₆, and [Pd(MeEt₄dien)Cl]Cl were investigated. The sulfite ion reaction follows the same first-order path as found previously for other ligands with this substrate, yet the thiosulfate ion reactions are described by both a ligand-dependent and a ligand-independent path. The kinetics of the reaction of [Pd(Et₄dien)H₂O](ClO₄)₂ with a series of nucleophiles was studied by the stopped-flow method; all reactions were fast and were first order in both substrate and reagent.

Introduction

The rates of substitution reactions of the sterically hindered complexes Pd(amine)X⁺ (amine = Et₄dien, MeEt₄dien, or Me₅dien; X = Cl or Br) with various nucleophiles have been shown to be independent of the concentration of entering nucleophile, even for good nucleophiles such as I^- and SCN^-.[2] This type of kinetic behavior is similar to that for octahedral com-

(1) dien = HN(C₂H₄NH₂)₂; Et₄dien = HN[C₂H₄N(C₂H₅)₂]₂; MeEt₄dien = CH₃N[C₂H₄N(C₂H₅)₂]₂; Me₅dien = CH₃N[C₂H₄N(CH₃)₂]₂.
(2) W. H. Baddley and F. Basolo, *J. Am. Chem. Soc.*, **88**, 2944 (1966).

plexes and was explained by a solvent-assisted dissociative mechanism

$$Pd(amine)X^+ + H_2O \xrightarrow{\text{slow}} Pd(amine)H_2O^{2+} + X^- \quad (1)$$

$$Pd(amine)H_2O^{2+} + Y^{n-} \xrightarrow{\text{fast}} Pd(amine)Y^{(2-n)+} + H_2O \quad (2)$$

The one exception to this kinetic behavior occurs when the amine is Et₄dien and the nucleophile is hydroxide ion; in this case a hydroxide ion dependence is found. This was explained by postulating the removal of a